RSC Sustainability

ROYAL SOCIETY OF CHEMISTRY

COMMUNICATION

View Article Online
View Journal | View Issue

Cite this: *RSC Sustainability*, 2026, **4**, 2117

Received 3rd April 2026
Accepted 8th April 2026

DOI: 10.1039/d6su00193a

rsc.li/rscsus

CO_2-mediated conversion of furfuryl alcohol to 4-hydroxycyclopentanone and its toxicological assessment

Ana Franco,[a] Marie Garcia,[b] K. De Oliveira Vigier,[a] Julien Vignard,[b] Isabelle P. Oswald,[b] Frédéric Guegan,[a] Gladys Mirey*[b] and François Jérôme*[a]

Through a combined chemical-toxicological study, this report re-explores the Piancatelli rearrangement of furfuryl alcohol into 4-hydroxycyclopentenone (**4-HCP**), a key building block for the synthesis of bio-based solvents. In this context, we demonstrate that (1) in aqueous media, the addition of CO_2 results in a fivefold increase in the rate of the Piancatelli rearrangement of furfuryl alcohol to **4-HCP**, even at temperatures as low as 120 °C, and (2) **4-HCP** exhibits pronounced cyto- and genotoxicity, approximately 200 times higher than that of furfural. Based on these results, we recommend avoiding the isolation of **4-HCP** and instead converting it *in situ* into cyclopentanone or cyclopentanol, two identified safer downstream target chemicals through toxicological studies.

Sustainability spotlight

This work aims to demonstrate that biobased products are not inherently safe, as too often claimed, and particular care must be taken in the selection of target molecules in order to prevent hazardous human exposure. And the case of biobased **4-HCP** is a perfect illustration of this. This study aligns with four goals of UN's Sustainable Development Goals: SDG 3: good health and well-being (article contribution: reduce human exposure to hazardous chemicals), SDG 9: industry, Innovation and Infrastucture (article contribution: foster innovation in biobased industry), SDG 12: responsible consumption and production (article contribution: design less toxic and biobased chemicals) and SDG 13: climate action (article contribution: reduce CO_2 emission by (i) improving the rate of reaction and (ii) lowering temperature of reaction).

The growing societal awareness of environmental challenges, such as global warming, health impacts, and resource depletion, has become a key driver of the transition from fossil-based to renewable feedstocks.[1] In this context, considerable efforts have been made in recent years to produce chemicals from biomass waste.[2] At the academic level, performance criteria or metrics such as reactor productivity, selectivity, catalyst consumption, CO_2 emissions, waste generation, life cycle assessment, among others, are commonly employed to evaluate the viability and scalability of biobased processes.[3] In contrast, the toxicity of biobased chemicals is far less frequently addressed, except at industrial scale, despite its critical importance in determining the market potential of a given chemical.

Furfural is one the few chemicals produced on a large scale (300 kT per year), and at a competitive price (1.5–2.5 €/kg), from biomass waste. As a result, furfural has emerged as a promising biobased building block for the synthesis of a wide range of downstream products, including aromatics, amphiphiles, hydrocarbons for instance, with applications in different end-industries such as cosmetics, automotive, electronics, packaging among others.[4] In most of these reaction pathways, 4-hydroxy-2-cyclopentenone (**4-HCP**) is often a key intermediate from which it is possible to create molecular complexity and diversity. For instance, **4-HCP** is the main intermediate in the conversion of furfural to cyclopentenone,[5] cyclopentanone,[6] cyclopentanol,[7] cyclopentanediol,[8] and cyclopentane,[9] all of which exhibit strong market potential as substitute to hazardous fossil-derived solvents across a variety of industries.[10] In these examples, furfural is converted over bifunctional acid/redox catalysts, with **4-HCP** as a central intermediate.[5–10]

4-HCP is typically obtained *via* the Piancatelli rearrangement of furfuryl alcohol (FOL),[11] the latter being the primary product in the catalytic hydrogenation of furfural.[12] Recently, in collaboration with Zhang, we demonstrated that the addition of CO_2 during the hydrogenation of furfural over Ru supported on CMK-3 (an ordered mesoporous carbon) led to the formation of 1,4-pentanediol, with **4-HCP** generated *in situ* as a key intermediate.[13] Inspired by this work, we now report a safety-by-design approach including (1) the effect of CO_2 on the conversion of FOL into **4-HCP** and (2) a toxicological assessment of **4-HCP**, and its downstream products, to assess the safety of this pathway and also to identify the most suitable biobased chemical to which **4-HCP** should ideally be converted into.

[a]*Institut de Chimie des Milieux et Matériaux de Poitiers, CNRS, Université de Poitiers, 1 Rue Marcel Doré, 86073 Poitiers, France. E-mail: francois.jerome@univ-poitiers.fr*
[b]*TOXALIM, INRAE, 180 Chemin de Tournefeuille, 31070 Toulouse Cedex 3, France. E-mail: gladys.mirey@inra.fr*

Surprisingly, despite previous reports on **4-HCP**, there is almost no information available about its toxicological profile.

Piancatelli rearrangement of FOL to 4-HCP under CO_2

The Piancatelli rearrangement of FOL to **4-HCP** proceeds under acid conditions *via* the intermediate formation of 4-oxopent-2-enal, which can undergo an intramolecular cyclization to **4-HCP** (Scheme 1, route 1). This pathway competes with the side sequential rehydration-dehydration of 4-oxopent-2-enal leading to the formation of levulinic acid (Scheme 1, route 2).[14] In addition, the intermediates can undergo uncontrolled reactions with each other, forming soluble and insoluble tar-like polycondensation products commonly referred to as humins.[5–10,15] Literature reports suggest that weak acids favor the formation of **4-HCP** over levulinic acid. Although the reason behind this observation is not fully understood, this is likely due to their inability to catalyze the hydration of the intermediate 4-oxopent-2-enal to levulinic acid. In most reported syntheses of **4-HCP**, weak acidity is generated *in situ* by conducting the reaction in pressurized hot water (~200 °C), where the autodissociation of water provides the required proton,[16] typically affording <60% yield of **4-HCP**. Alternatively, adding weak acids such as carboxylic acids (*e.g.*, acetic or levulinic acid) can promote the reaction at lower temperatures (around 160 °C), although the recyclability of these catalysts still represents a major challenge.[5b]

In our combined chemical-toxicological methodology, we first investigated in more detail the role of CO_2 as a catalyst in the Piancatelli rearrangements of FOL to **4-HCP**. In water, CO_2 forms carbonic acid, a weak acid that reduces the solution pH. Advantageously, at the end of the reaction, depressurization converts carbonic acid back into CO_2 and H_2O, providing an elegant alternative to the challenging recovery and regeneration of conventional acid catalysts, which are often deactivated by humin deposition. This approach also prevents contamination of the reaction products with acid catalyst residues, which can significantly affect their downstream transformations.

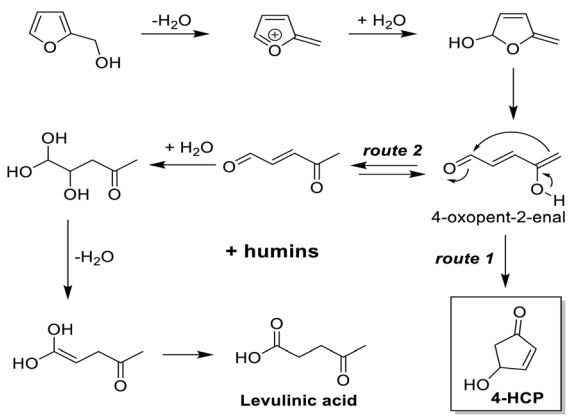

Scheme 1 Simplified mechanism illustrating the conversion of FOL to either levulinic acid or **4-HCP**.

In a first series of experiments, we examined the thermal (*i.e.* CO_2-free) conversion of FOL to **4-HCP** in the 120–200 °C temperature range. These experiments serve as benchmark reactions for this study. Reactions were carried out in a biphasic D_2O/methyl tetrahydrofuran (60 : 40) system in order to tentatively limit the formation of humins by preferentially partitioning **4-HCP** into the organic phase. D_2O was employed instead of H_2O to enable reaction monitoring by ^1H NMR (Fig. S1). All experiments were performed in an autoclave under air with a heating ramp of 3.45 °C min^{-1} (ESI). The corresponding results are summarized in Fig. 1. In agreement with previous reports in hot water, within 1 h of reaction time, nearly complete conversion of FOL was observed only when the temperature was set over 180 °C. Increasing the temperature up to 200 °C even resulted in an improvement in **4-HCP** selectivity at total conversion (79 *vs.* 65% at 180 and 200 °C, respectively). Extending the reaction time to 70 min at 200 °C after complete conversion of FOL did not further enhance the yield or selectivity. Instead, **4-HCP** started to be slightly decomposed, indicating that the maximum attainable yield had been reached after 1 h. Under these conditions, no levulinic acid was detected by HPLC or ^1H NMR, and the by-products mainly consisted of humins, very common side products observed in the thermal conversion of FOL. So far, the structures of these humins are rather complex to determine and, based on the existing literature, they mainly consist of polycondensed furanic derivatives through ring opening, Diels–Alder reactions, *etc.*[15] Formation of humins is evidenced in our case by the formation of black soluble and insoluble tar-like materials (Fig. S2). An Arrhenius plot (logarithm of the **4-HCP** formation rate *versus* inverse temperature) afforded an activation energy of ~50 kJ mol^{-1} (Fig. S3).

To improve reaction rate at lower temperatures, and inspired by our previous work on the acid-catalyzed conversion of sugars to furanic derivatives,[17] CO_2 was introduced into the reactor to

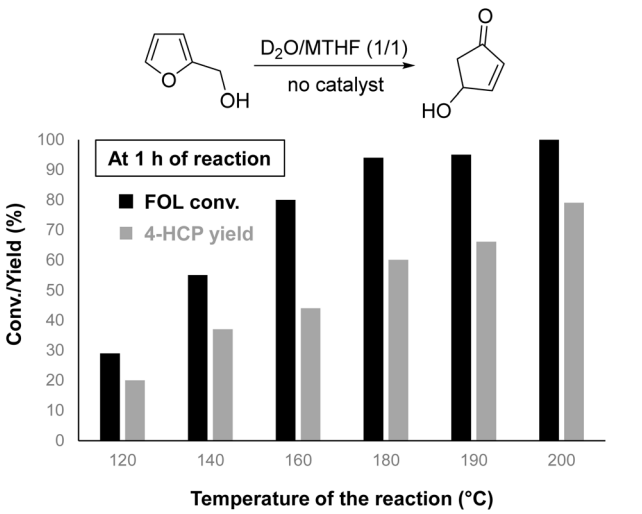

Fig. 1 Effect of the temperature on the thermal conversion of FOL to **4-HCP** (data were collected after 1 h of reaction, 3 wt% of FOL in 19 mL of a 60/40 D_2O/MTHF biphasic mixture).

form *in situ* carbonic acid, a Brønsted acid catalyst. As discussed above, at 120 °C and under purely thermal conditions, the reaction proceeds slowly, requiring approximately 8 hours to reach a 62% yield of **4-HCP** (Fig. 2A). Remarkably, the introduction of 20 bar of CO_2 into the reactor afforded **4-HCP** in 52% yield after just 1 h of reaction, corresponding to an almost fivefold increase in the rate of conversion of FOL as compared to purely thermal conditions (Fig. 2A). Although *in situ* pH measurements during the reaction were challenging at 20 bar, we observed a drop in pH to approximately 3.5 at the end of the reaction, supporting acidification of the reaction medium with CO_2. Similar enhancements in FOL conversion were observed at 140 and 160 °C (Fig. 2B). For example, without CO_2, it takes 2 hours to reach 61% and 100% conversion of FOL at 140 and 160 °C, respectively, whereas in the presence of 20 bar CO_2, the same conversions are achieved in only 30 minutes (140 °C) and 5 minutes (160 °C) (Table S2 and Fig. S4). An Arrhenius plot under CO_2 revealed a dramatic reduction in the activation energy to <10 kJ mol^{-1}, highlighting the significant promoting effect of CO_2 on this reaction (Fig. S3).

Increasing the CO_2 pressure from 10 to 20 bar resulted in a 3.5-fold rise in the initial conversion rate of FOL, presumably due to a higher acidification of the reaction media. However, further raising the CO_2 pressure to 30 bar had minimal impact on either the reaction rate or selectivity, suggesting that 20 bar is sufficient to saturate the solution with carbonic acid (Table S3 and Fig. S5).

To confirm that CO_2 acts as a Brønsted acid catalyst, *i.e. via* the formation of H_2CO_3 upon dissolution in water, similar experiments were carried out using various Lewis and Brønsted acid catalysts (Table 1). In the presence of 15 mol% of Lewis acids such as $ZnCl_2$ or ZnI_2 at 120 °C, FOL was converted to **4-HCP** in only 27% and 29% yield, respectively, after 2 h (Table 1, entries 2, 3). Compared with the reaction conducted in the absence of catalyst at 120 °C (Fig. 2A and Table 1, entry 4), this corresponds to a negligible improvement in **4-HCP** formation rate and selectivity, indicating that these Lewis acid salts do not effectively catalyze the reaction. This conclusion was further supported by increasing the dosage of $ZnCl_2$ from 15 to 50 mol%, which had no impact on the conversion rate (Table 1, entry 5). In contrast, when 15 mol% of acetic acid was used as a Brønsted acid catalyst, similar improvements in both reaction rate and selectivity to **4-HCP** to those observed with CO_2 were observed (Table 1, entry 6). Taken together, these results support the conclusion that CO_2 indeed behaves as a Brønsted acid under our reaction conditions, with the additional advantage that it can be readily removed at the end of the reaction by simple depressurization of the reactor. To definitely support this claim, **4-HCP** selectivity was plotted as a function of FOL conversion, both with Brønsted acid (CO_2 and acetic acid) and without. Interestingly, in the absence of Brønsted acid, selectivity remained around 65% regardless of conversion, whereas in the presence of Brønsted acid catalysts selectivity increased with conversion, reaching a similar value (~65%) only at near-complete conversion (~90%) (Fig. S6). This change in selectivity behavior strongly supports a better stabilization of reaction intermediates in the presence of Brønsted acid catalysts, which are subsequently transformed into **4-HCP** over time.

A first set of DFT calculations was carried out to clarify the possible reaction pathway at play under CO_2, and more largely with Brønsted acid catalyst. We initially considered the possible involvement of CO_2 in the final step of the reaction (ring closure from 4-oxopent-2-enal), since two formal chemical events are expected to occur simultaneously: a proton transfer and a pericyclic electron shift. These calculations showed that carbonic acid, and even formic acid used here as another model Brønsted acid, could act as proton shuttles to facilitate the cyclization

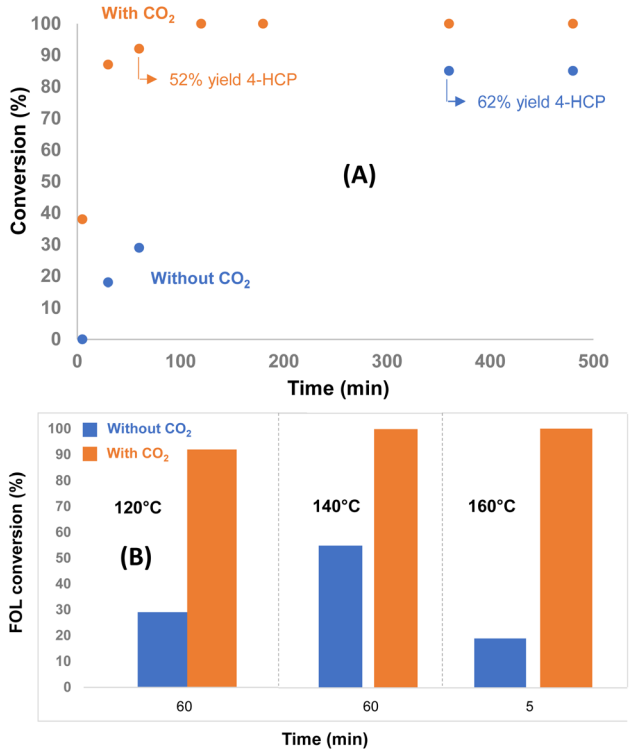

Fig. 2 (A) Comparison of FOL conversion rate without (blue) and with (orange) CO_2 at 120 °C and (B) comparison of FOL conversion rate enhancement at 120, 140 and 160 °C.

Table 1 Conversion of FOL to **4-HCP** in the presence of different Brønsted and Lewis acid catalysts

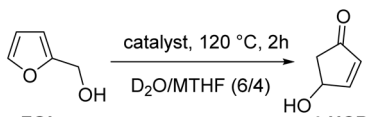

Entry	Acid catalyst[a]	Time (min)	Conv. (%)	Yield (%)	Selectivity (%)
1	CO_2	60	92	52	57
2	$ZnCl_2$	120	41	27	66
3	ZnI_2	120	47	29	62
4	—	120	45	32	72
5	$ZnCl_2$[b]	120	40	20	50
6	Acetic acid	60	90	66	73

[a] 15 mol%. [b] 50 mol%.

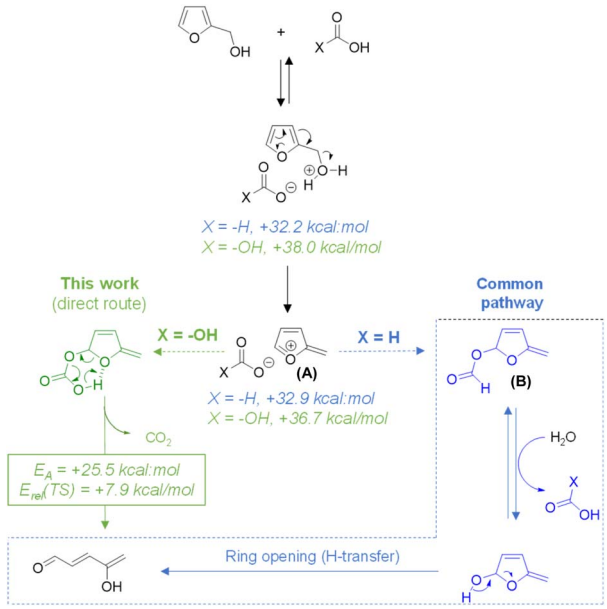

Scheme 2 Schematic representation of the formation of 4-oxopent-2-enal from the reaction of FOL with either formic acid (X = −H, blue) or carbonic acid (X = −OH, green) as studied by DFT calculations at the wB97xD/6-311++G(d,p) + PCM(H_2O) level of theory. ZPE-corrected energies are given relative to the starting reagents.

reaction, lowering the activation energy by 12–13 kcal mol^{-1} (see SI for details). We then considered whether CO_2 might also intervene earlier along the reaction pathway, prior to the formation of 4-oxopent-2-enal. Formally, the acid-catalyzed dehydration of FOL requires a proton transfer, generating a transient $FOLH^+$ species that can then spontaneously dehydrate to produce the carbocation (A) depicted in Scheme 2. In the presence of formic acid, the intermediate (A) may subsequently be trapped by the conjugate base of the catalyst, resulting in the formation of the adduct (B) which would unavoidably require an additional hydrolysis step to yield 4-oxopent-2-enal. Interestingly, with CO_2, an alternative pathway was identified which directly afford 4-oxopent-2-enal through a concerted proton-transfer/decarboxylation/ring-opening process. Pleasingly, calculations showed that the ion pairs indeed give rise to stable intermediates, and that a transition state for this concerted proton-transfer/decarboxylation/ring-opening step can be located in the case of bicarbonate, lying 25.5 kcal mol^{-1} above the intermediate, but only 0.5 kcal mol^{-1} above the separated ions and 7.9 kcal mol^{-1} above the starting reagents (thus implying a rather modest energetic cost). Overall, these results suggest that the peculiarity of CO_2 may stem from its dual ability to act as both a proton and a formal "oxygen-atom" shuttle (or alternatively as an activator of water).

Safety-toxicological studies

Although the use of CO_2 speed-up the production of **4-HCP** from FOL, questions remain regarding the cytotoxicity of this biobased compound, a critical factor for evaluating its market potential. To date, if furanoids toxicity is well documented,[18] the cytotoxicity of **4-HCP** has not been reported yet. To address this, its effects were investigated *in vitro* using two human model cell lines largely used in toxicology: the Caco-2 intestinal cells as a biological barrier model and HepG2 hepatic cells for metabolic activities (ESI).

For this purpose, each cell line was exposed to various concentrations of furfural, FOL or **4-HCP** for 24 hours (Fig. S7A). To evaluate the effects of acute exposure over a longer period, a pulse-chase experiment was performed, consisting of a 24 hours exposure followed by a culture-medium change and an additional 24 hours incubation (Fig. S7B). A clear dose-dependent response was observed after 24 hours of treatment, with **4-HCP** causing a 50% loss of viability, *i.e.* IC_{50} at 50 μM on both cells lines after 24 hours of exposure (Fig. S7A). In comparison, FOL induced no loss of viability at 1 mM after 24 hours of exposure. At the later timepoint, the total loss of viability is observed at 50 μM of **4-HCP**, both for hepatic or intestinal cells. Again, no loss of viability was observed for 1 mM of FOL (Fig. S7B). Thus **4-HCP** appears at least 200 times more cytotoxic than FOL or its precursor furfural (FA) when comparing IC_{50}. In addition, Caco-2 cells are as sensitive as HepG2 cells to **4-HCP**, suggesting that the proliferation rate or the capacity to metabolize **4-HCP** are not involved in this cytotoxic effect (Table S4). Overall, these results highlight the high toxicity of **4-HCP** in the micromolar range (Fig. 3).

The mechanism underlying the cytotoxicity was investigated using an oxidative stress assay (ESI). For this purpose, furfural, FOL, or **4-HCP** were each incubated for 24 hours with HepG2 or Caco-2 cell lines. The oxidative stress was quantified within the nuclei of cells exposed to **4-HCP** in comparison with FA and FOL, as well as negative and positive controls (Fig. S8). **4-HCP** induced a strong nuclear oxidative stress, this effect being already detectable after only 4 hours of exposure. In comparison, 1000 times higher concentrations of FA and FOL induced a lower oxidative stress. Altogether, these findings suggest that the cytotoxicity of **4-HCP** may result from an important oxidative stress occurring after cellular exposure. Because oxidative stress can lead to damage of cellular genetic material (DNA), we also examined the effect of acute exposure on DNA integrity (ESI). The γH2AX biomarker of DNA damage was used and quantified, compared to the negative and positive controls, and expressed as fold-change relative to the negative control (Fig. S9). After 24 hours of exposure at 40 μM, **4-HCP** induced a strong γH2AX signal, indicating that the oxidative stress triggered by **4-HCP** is also accompanied by genotoxic stress.

Taken together, these results highlight the high cyto- and genotoxicity of **4-HCP**, which is higher than that of the starting material FOL. This finding underscores the need for caution when handling **4-HCP** as a biobased building block. From a chemical standpoint, it suggests that **4-HCP** should not be isolated but instead converted *in situ* into downstream products to minimize potential human exposure. One possible strategy is the *in situ* conversion of **4-HCP** into cyclopentenone (CP-ENONE), cyclopentanone (CP-ANONE), cyclopentanol (CP-ANOL), or cyclopentane (CP-ANE), all of which are biobased solvents with significant market potential. Starting from FOL, or even from furfural, this transformation has been reported

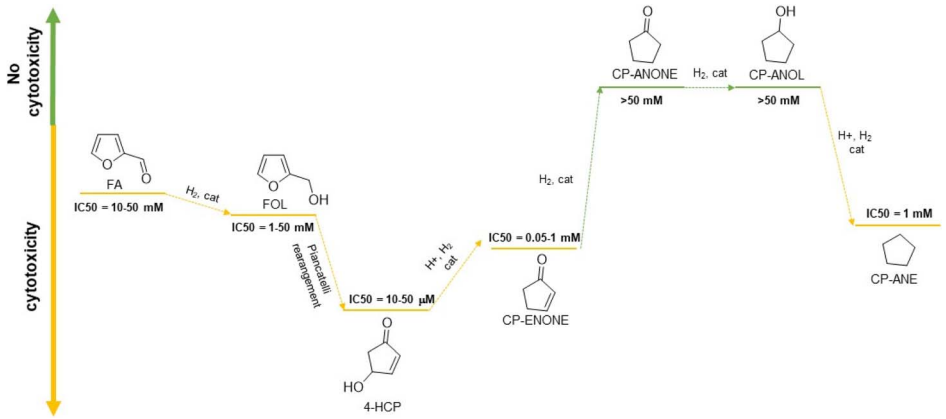

Fig. 3 Toxicological profile of **4-HCP**, its precursor and its downstream products.

feasible in the literature and typically proceeds through two steps: (1) conversion of FOL to **4-HCP**, followed by (2) its *in situ* transformation into CP-ENONE/CP-ANONE/CP-ANOL/CP-ANE *via* a cascade of hydrodeoxygenation reactions over bifunctional acid/redox catalysts.[5–10] To determine which downstream product **4-HCP** should ideally be converted into, we conducted additional cytotoxicity assays on hydrodeoxygenated derivatives obtained from **4-HCP** (Fig. S7). *In vitro*, CP-ENONE was found to be more cytotoxic, with a 50% loss of viability at 100 µM on hepatic HepG2 cells at the later point, approximately 100 times more toxic than FOL, making it an undesirable downstream target. A similar conclusion can be drawn for the fully hydrodeoxygenated CP-ANE (Fig. 3). In contrast, CP-ANONE and CP-ANOL showed cytotoxicity over 50 mM in both tested cell lines, being less cytotoxic than the starting FOL (Fig. 3). Overall, these findings indicate that **4-HCP** should ideally be converted *in situ* into CP-ANONE or CP-ANOL to avoid hazardous exposure risks to humans.

Conclusions

We report that CO_2 catalyzes the conversion of FOL to **4-HCP**. Under optimized conditions, **4-HCP** was obtained in 62% yield in about 1 h at only 120 °C. While further studies are needed to fully elucidate the reasons behind these results obtained with CO_2, DFT calculations and experiments highlighted that CO_2 behaves as a Brønsted acid catalyst, *via* the formation of H_2CO_3 upon dissolution in water. Interestingly, unlike commonly used Brønsted acid catalysts such as formic acid, CO_2 can also promote a competing alternative pathway leading to the intermediate 4-oxopent-2-enal, *via* a concerted proton transfer, decarboxylation, and ring-opening process.

Despite its synthetic potential, we demonstrated that **4-HCP** is highly cyto- and genotoxic, about 200 times more than FOL and above for furfural. Therefore, **4-HCP** should not be isolated but rather converted *in situ* to safer downstream products to avoid human exposure. In this context, we identified *in situ* conversion of **4-HCP** to cyclopentanone or cyclopentanol as a safer option from a toxicological perspective.

Ongoing work in our group focuses on extending this approach to the CO_2-assited catalytic conversion of furfural to cyclopentanone or cyclopentanol.

Author contributions

A. Franco performed all experimental tests with and without CO_2. F. Guegan was in charge of theoretical calculations. K. De Oliveria Vigier and F. Jérôme co-supervised the work. For toxicological analysis, M. Garcia was involved in methodology, investigation and formal analysis; J. Vignard in formal analysis, review & editing; I. P. Oswald in funding acquisition, conceptualization, review & editing; G. Mirey Project administration/supervision, conceptualization, formal analysis, writing, review & editing.

Conflicts of interest

There are no conflicts to declare.

Data availability

The data supporting this article have been included as part of the supplementary information (SI). Supplementary information is available. See DOI: https://doi.org/10.1039/d6su00193a.

Acknowledgements

The authors thank L. Chaib for preliminary results. The authors gratefully acknowledge the CNRS and the University of Poitiers for their financial support. The authors also acknowledge financial support from the European Union (ERDF) and Région Nouvelle Aquitaine. The authors further extend their thanks to France 2030 for funding the ECOCHEM (ANR-22-PESP-0006) and FURFUN (ANR-22-PEBB-0007) projects, within which this study was carried out.

Notes and references

1 (*a*) J.-P. Lange, *Energy Environ. Sci.*, 2021, **14**, 4358–4376; (*b*) G. Lopez, D. Keiner, M. Fasihi, T. Koiranen and C. Breyer, *Energy Environ. Sci.*, 2023, **16**, 2879–2909.

2 (*a*) J. J. Bozell and G. R. Petersen, *Green Chem.*, 2010, **12**, 539–554; (*b*) Z. Zhang, J. Song and B. Han, *Chem. Rev.*, 2017, **117**(10), 6834–6880; (*c*) S. Venkata Mohan, G. N. Nikhil, P. Chiranjeevi, C. Nagendranatha Reddy, M. V. Rohit, A. Naresh Kumar and O. Sarkar, *Biores. Technol.*, 2016, **215**, 2–12; (*d*) G. W. Huber, S. Iborra and A. Corma, *Chem. Rev.*, 2006, **106**(9), 4044–4098; (*e*) R. Mori, *RSC Sustain.*, 2023, **1**, 179–212.

3 (*a*) J.-P. Lange, *Nature Catal*, 2021, **4**, 186–192; (*b*) S. Kim and M. Overcash, *J. Chem. Technol. Biotechnol.*, 2003, **78**, 995–1005.

4 J.-P. Lange, *Catal. Today*, 2024, **435**, 114726.

5 (*a*) X. Li, Q. Deng, L. Yu, R. Gao, Z. Tong, C. Lu, J. Wang, Z. Zeng, J.-J. Zou and S. Deng, *Green Chem.*, 2020, **22**, 2549–2557; (*b*) M. Hronec, K. Fulajtárová and T. Soták, *J. Ind. Eng. Chem.*, 2014, **20**, 650–655.

6 (*a*) R. Baldenhofer, J.-P. Lange, S. R. A. Kersten and M. P. Ruiz, *ChemSusChem*, 2024, **24**, e202400108; (*b*) Y. Yang, Z. Du, Y. Huang, F. Lu, F. Wang, J. Gao and J. Xu, *Green Chem.*, 2013, **15**, 1932–1940; (*c*) M. Hronec, K. Fulajtárova and T. Soták, *App. Catal. B: Environ.*, 2014, **154–155**, 294–300; (*d*) M. Dohade and P. L. Dhepe, *Catal. Sci. Technol.*, 2018, **8**, 5259–5269; (*e*) M. Hronec and K. Fulajtarová, *Catal. Commun.*, 2012, **24**, 100–104; (*f*) J. Guo, G. Xu, Z. Han, Y. Zhang, Y. Fu and Q. Guo, *ACS Sust. Chem. Eng.*, 2014, **2**, 2259–2266.

7 (*a*) L. Liu, Y. Si, W. Zhao, Q. Zhu, Z. Yang, J. He, Y. Huang and Y. Cheng, *ChemCatChem*, 2024, **16**, e202401085; (*b*) H. Li, M. Luo, T. Zhu, C. Wang, Y. Liao, H. Wang and L. Ma, *App. Catal. B: Environ.*, 2025, **366**, 125052; (*c*) X. Zhou, Z. Feng, W. Guo, J. Liu, R. Li, R. Chen and J. Huang, *Ind. Eng. Chem. Res.*, 2019, **58**(10), 3988–3993; (*d*) H. Li, M. Luo, T. Zhu, C. Wang, Y. Liao, H. Wang and L. Ma, *Appl. Catal. B: Environ.*, 2025, **366**, 125052.

8 G. Li, N. Li, M. Zheng, S. Li, A. Wang, Y. Cong, X. Wang and T. Zhang, *Green Chem.*, 2016, **18**, 3607–3613.

9 (*a*) A. Bredihhin, S. Salmar and L. Vares, *ACS Omega*, 2018, **3**(8), 10211–10215; (*b*) H. Li, M. Luo, T. Zhu, C. Wang, Y. Liao, H. Wang and L. Ma, *Appl. Catal. B: Environ.*, 2025, **366**, 125052.

10 (*a*) G. König, P. Hauk and F. Gallou, *RSC Sustain.*, 2025, **3**, 1539–1549; (*b*) X. Yue and Y. Queneau, *ChemSusChem*, 2022, **15**(13), e202102660.

11 (*a*) G. Piancatelli, A. Scettri and S. Barbadoro, *Tet. Lett.*, 1976, **17**, 3555–3558; (*b*) C. Piutti and F. Quartieri, *Molecules*, 2013, **18**, 12290–12312.

12 A. Jaswal, P. P. Singh and T. Mondal, *Green Chem.*, 2022, **24**, 510–551.

13 F. Liu, Q. Liu, J. Xu, L. Li, Y.-T. Cui, R. Lang, L. Li, Y. Su, S. Miao, H. Sun, B. Qiao, A. Wang, F. Jérôme and T. Zhan, *Green Chem.*, 2018, **20**, 1770–1776.

14 (*a*) S. An, D. Song, Y. Sun, Q. Zhang, P. Zhang and Y. Guo, *ACS Sust. Chem. Eng.*, 2018, **6**(3), 3113–3123; (*b*) G. M. González Maldonado, S. Assary, J. Dumesic and L. A. Curtiss, *Energy Environ. Sci.*, 2012, **5**, 6981–6989; (*c*) V. W. Faria, K. M. A. Santos, A. M. Calazans and M. A. Fraga, *ChemCatChem*, 2023, **15**(15), e202300447; (*d*) L. Fuentes-Rodriguez, A. Le Corre and Y. Cesteros, *Appl. Catal. A: Gen.*, 2025, **698**, 120238.

15 E. de Jong, M. Mascal, S. Constant, T. Claessen, P. Tosi and A. Mija, *Green Chem.*, 2025, **27**, 3136–3166.

16 G. Arcile, J. Ouazzani and J.-F. Betzer, *React. Chem. Eng.*, 2022, **7**, 1640–1649.

17 (*a*) F. Liu, J. Barrault, K. de Oliveira Vigier and F. Jérôme, *ChemSusChem*, 2012, **5**(7), 1223–1226; (*b*) F. Liu, M. Audemar, K. De Oliveira Vigier, J.-M. Clacens, F. De Campo and F. Jérôme, *ChemSusChem*, 2014, **7**(8), 2089–2093; (*c*) M. Audemar, L. Atencio-Gene, C. Ortiz Mellet, F. Jérôme, J. García Fernández and K. De Oliveira Vigier, *J. Agric. Food Chem.*, 2017, **65**(30), 6093–6099.

18 Y.-K. Lin, C.-Y. Hsiao, C.-J. Chen, A. Alalaiwe, C. Lee, T.-H. Huang and J.-Y. Fang, *Environ. Res.*, 2024, **261**, 119757.